

Lawrence Berkeley National Laboratory

Recent Work

Title

Surface Studies by Nonlinear Optics

Permalink

<https://escholarship.org/uc/item/46b1g87z>

Authors

Xiao, X.D.

Shen, Y.R.

Publication Date

1992-12-01



Lawrence Berkeley Laboratory
UNIVERSITY OF CALIFORNIA

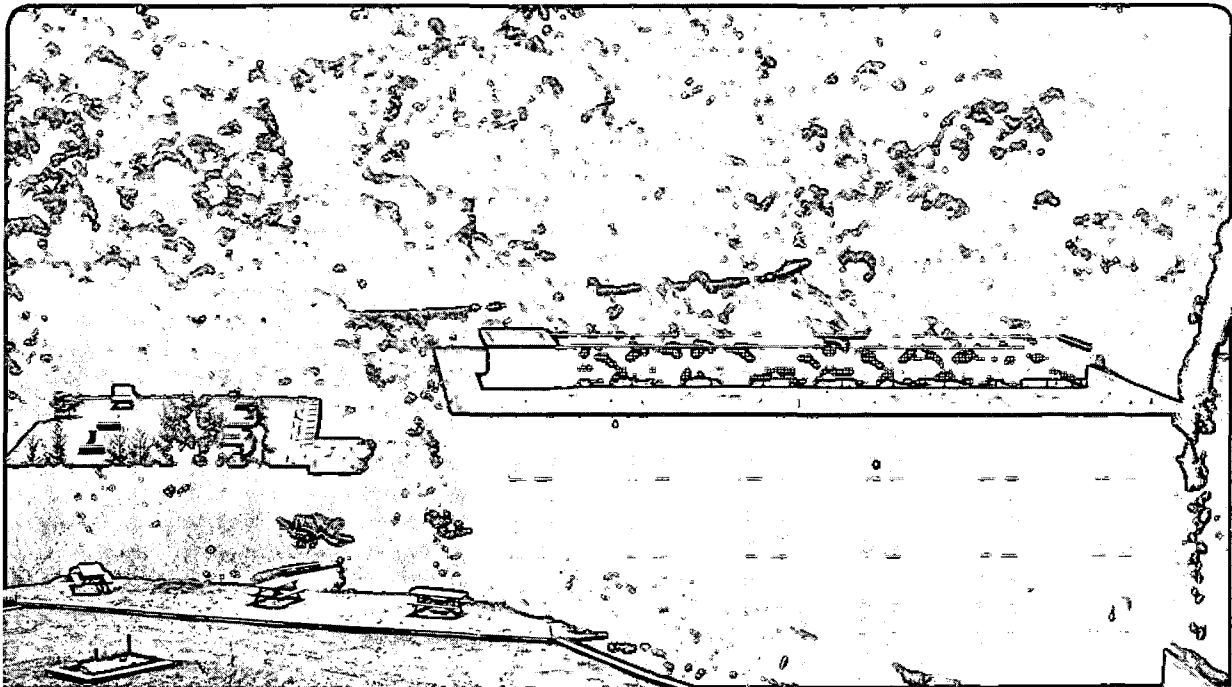
Materials Sciences Division

Presented at the Society of Photo-Optical Instrumentation Engineers,
Los Angeles, CA, January 19-21, 1993, and to be published
in the Proceedings

Surface Studies by Nonlinear Optics

X.-D. Xiao and Y.R. Shen

December 1992



LBL-33384

DISCLAIMER

This document was prepared as an account of work sponsored by the United States Government. While this document is believed to contain correct information, neither the United States Government nor any agency thereof, nor the Regents of the University of California, nor any of their employees, makes any warranty, express or implied, or assumes any legal responsibility for the accuracy, completeness, or usefulness of any information, apparatus, product, or process disclosed, or represents that its use would not infringe privately owned rights. Reference herein to any specific commercial product, process, or service by its trade name, trademark, manufacturer, or otherwise, does not necessarily constitute or imply its endorsement, recommendation, or favoring by the United States Government or any agency thereof, or the Regents of the University of California. The views and opinions of authors expressed herein do not necessarily state or reflect those of the United States Government or any agency thereof or the Regents of the University of California.

LBL-33384
UC410

Surface Studies by Nonlinear Optics

Xu-dong Xiao and Y. R. Shen

Department of Physics
University of California

and

Materials Sciences Division
Lawrence Berkeley Laboratory
University of California
Berkeley, California 94720

December 1992

This work was supported by the Director, Office of Energy Research, Office of Basic Energy Sciences, Materials Sciences Division, of the U.S. Department of Energy under Contract No. DE-AC03-76SF00098.

Surface Studies by Nonlinear Optics

Xu-dong Xiao, and Y. R. Shen

Department of Physics, University of California
Materials Sciences Division, Lawrence Berkeley Laboratory
Berkeley, California 94720

ABSTRACT

Optical second harmonic generation (SHG) has been widely employed as a surface probe. Applications of the technique to adsorption, desorption, surface diffusion, molecular orientation and surface chemistry of adsorbed molecules are described as examples. Surface SHG and sum frequency generation (SFG) for surface spectroscopic studies are also described.

I. INTRODUCTION

Although second harmonic generation (SHG) was discovered soon after laser was invented, its use as a surface probe was developed more recently¹. Since then, the technique has been employed to study a variety of surface processes. For example, it has been used to study adsorption, desorption and surface diffusion of adsorbates on well defined surfaces in ultrahigh vacuum. For molecules at air/liquid and air/solid interfaces, it has been adopted to study molecular orientation and alignment of adsorbates. With tunable lasers, SHG and surface sum frequency generation (SFG) have been used for spectroscopic studies of surface states and surface molecular vibrations.

As a second-order nonlinear optical effect, SHG and SFG are forbidden under the electric-dipole approximation in a medium with inversion symmetry. At the surface or interface, the inversion symmetry is broken and the processes become allowed. They are therefore highly surface-specific. Moreover, they have a submonolayer sensitivity and are extremely versatile as a surface probe. First, they are applicable to all interfaces accessible to light. Second, they have inherently high spatial, temporal and spectral resolutions. With ultrashort, tunable pulses, time-resolved surface spectroscopy and ultrafast surface dynamics can be studied.

In this paper we shall discuss a few recent applications of surface SHG and SFG. Section II describes the probing of surface adsorption, desorption and surface diffusion of adsorbed molecules on well defined surfaces using SHG. Section III discusses how surface molecular orientation and surface chemistry can be investigated by SHG. Section IV illustrates the potential of SHG and SFG for surface spectroscopy studies.

II. ADSORPTION, DESORPTION AND DIFFUSION

Adsorption of atoms or molecules on surfaces is one of the most important basic processes in surface science. SHG is capable of *in situ* monitoring of the adsorption process. The signal comes from three different contributions: the bare substrate, the adsorbates, and the interaction between the substrate and adsorbates. In terms of the surface second-order susceptibility, we have

$$\chi_s^{(2)}(\theta) = \chi_{ss}^{(2)} + \chi_m^{(2)}(\theta) + \chi_i^{(2)}(\theta). \quad (1)$$

where θ is the surface coverage of the adsorbates. With atoms or small molecules as adsorbates, the

adsorbate contribution $\chi_m^{(2)}(\theta)$ is usually negligible and the coverage dependence of $\chi_s^{(2)}(\theta)$ is mainly from the interaction part $\chi_i^{(2)}(\theta)$. If the adsorbate-substrate interaction can be treated locally and the interaction between adsorbates is negligible, we can write,

$$\chi_s^{(2)}(\theta) = A + B\theta, \quad (2)$$

with A and B being coverage-independent constants. This is the case for CO/Ni(111). Figure 1 shows the SH signal as a function of CO exposure for *in situ* monitoring of CO adsorption on Ni(111)². As seen in the figure, the result can be fit by the Langmuir kinetics with a time dependent coverage $\theta(t) = \theta_s(1 - e^{-\gamma t})$, where θ_s is the saturation coverage and γ is an adjustable parameter.

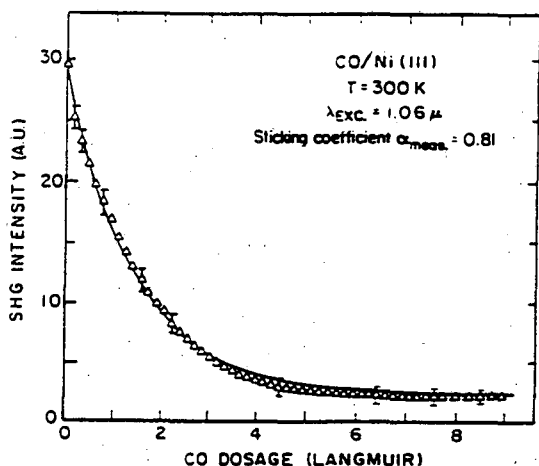


Fig. 1 Second harmonic signal as a function of CO exposure for CO/Ni(111) at 300K. The solid theoretical curve derived from the simple Langmuir kinetics model is used to fit the experimental data (Δ)(after Ref. 2).

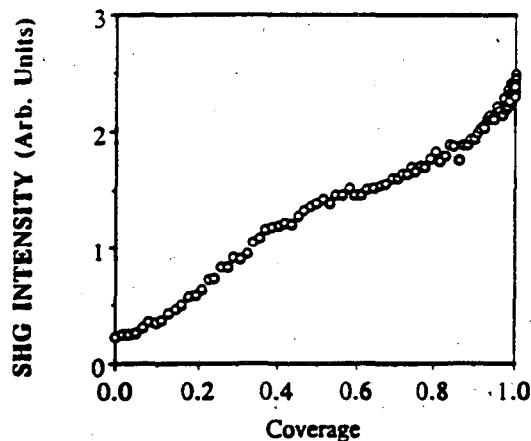


Fig. 2 Second harmonic signal as a function of coverage with the plane of incidence parallel to $[1\bar{1}0]$ and a p-in/p-out polarization combination for CO/Ni(110). (After Ref. 3).

We have to point out that the linear dependence of $\chi_s^{(2)}(\theta)$ on θ is an exception rather than a rule.

For most systems this simple relation may not hold. An example is given by Fig. 2 for CO/Ni(110)³. In this case, the SHG measurement can still provide information on adsorption kinetics if SHG has been calibrated against the coverage by other means. The technique is particularly useful for time-resolved *in situ* monitoring of an adsorption process.

SHG is ideal for measuring desorption kinetics if it is calibrated against coverage. It can be used to monitor the residual adsorbate coverage in a number of desorption modes, namely, temperature programmed thermal desorption (TDS), laser-induced-thermal-desorption and isothermal desorption. Although no particular advantage exists over normal TDS using a mass spectrometer, SHG is one of the few methods that can be employed to probe laser-induced-thermal-desorption and isothermal desorption. In a recent experiment, for example, Heinz *et al* used SHG to measure isothermal desorption of

H/Si(111) and H/Si(100)⁴. They found that the desorption of H from Si(111) is neither first order or second order (Fig. 3), but a mixture of the two. In such an experiment, mass spectroscopy for monitoring desorption is often unsuitable because of difficulty to discriminate against background desorption from the sample holder.

Surface diffusion of adsorbate is important for the understanding of phenomena such as catalysis, crystal growth, etc. It was recently demonstrated that SH diffraction from a monolayer grating can be a viable method to probe surface diffusion. It has been used to study CO diffusion on Ni(111) and Ni(110) surfaces. The scheme for the measurement is fairly straightforward. Two laser beams brought to overlap and create an interference pattern on a surface preadsorbed with molecules. The spatially modulated laser intensity is intense enough to desorb adsorbates and produce an adsorbate grating, which can be detected by SH diffraction of a third beam from the grating. When the grating gets smeared out as a result of surface diffusion, the diffraction signal decays correspondingly and the surface diffusion coefficient can be deduced. In the simplest case where $\chi_s^{(2)}(\theta)$ is linear with θ and the diffusion coefficient is independent of θ , the diffraction signal from a grating of spacing s is given by

$$S(t) = S_0 \exp(-8\pi^2 D t / s^2). \quad (3)$$

From which the diffusion coefficient D can be determined. A representative set of SH diffraction data is shown in Fig. 4 for CO diffusion on Ni(110) surface³.

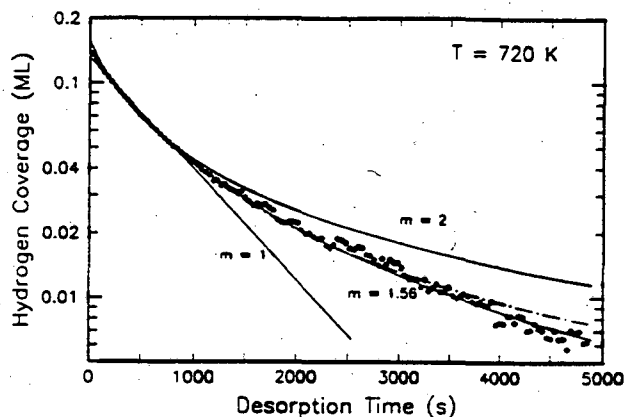


Fig. 3 Semilogarithmic plot of isothermal desorption of H₂ from Si(111)7x7 at a surface temperature of 720K and an

initial coverage of 0.14ML. The results are compared with best fits to simple first- and second-order kinetics and to an effective kinetic order of $m=1.56$. (After Ref. 4).

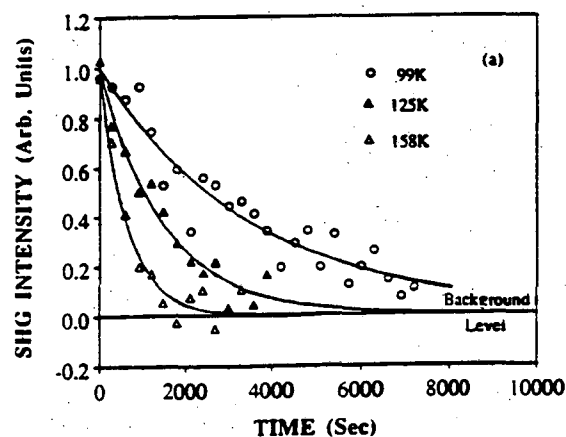


Fig. 4 Normalized first-order SH diffraction signal versus time at three different temperatures for CO diffusion along

[110] of Ni(110) surface. The solid lines are single exponential fits with Eq. (3) (After Ref. 3).

III. MOLECULAR ORIENTATION AND SURFACE CHEMISTRY

Surface SHG is applicable to any interface accessible by light. In particular, it can be used to study surfaces in air. We consider two examples here. The first one concerns measurements of orientations of adsorbed molecules on liquid or solid surfaces. The second one is a surface chemistry study of adsorbed molecules on a water surface.

For large molecules on water or glass surfaces, the contributions to SHG from the substrate and the interaction are much smaller than that from the molecules. The surface second order susceptibility can be written as

$$\chi_{s,ijk}^{(2)} = N_S \langle G_{ijk}^{\xi\eta\zeta} \rangle \alpha_{\xi\eta\zeta}^{(2)}, \quad (4)$$

with $\alpha_{\xi\eta\zeta}^{(2)}$ being the molecular polarizability tensor elements, $G_{ijk}^{\xi\eta\zeta}$ being a transformation from molecular coordinates (ξ, η, ζ) to the sample coordinates (i, j, k) , and the brackets $\langle \rangle$ being an average over the molecular orientation. For rod-like molecules, $\vec{\alpha}^{(2)}$ is often dominated by a single component $\alpha_{\zeta\zeta\zeta}^{(2)}$ along the long axis. If the adsorbates are distributed isotropically on a surface, the adsorbed monolayer should have a C_{∞} symmetry and the nonvanishing tensor elements of $\vec{\chi}_s^{(2)}$ are

$$\begin{aligned} \chi_{s,zzz}^{(2)} &= N_S \langle \cos^3 \theta \rangle \alpha_{\zeta\zeta\zeta}^{(2)}, \\ \chi_{s,zxx}^{(2)} = \chi_{s,zyy}^{(2)} = \chi_{s,xzx}^{(2)} = \chi_{s,yzy}^{(2)} &= \frac{1}{2} N_S \langle \sin^2 \theta \cos \theta \rangle \alpha_{\zeta\zeta\zeta}^{(2)}. \end{aligned} \quad (5)$$

If the distribution has a C_{1v} symmetry, the nonvanishing elements are

$$\begin{aligned} \chi_{s,zzz}^{(2)} &= N_S \langle \cos^3 \theta \rangle \alpha_{\zeta\zeta\zeta}^{(2)}, \\ \chi_{s,xxx}^{(2)} &= -N_S \langle \sin^3 \theta \rangle \langle \cos^3 \phi \rangle \alpha_{\zeta\zeta\zeta}^{(2)}, \\ \chi_{s,zxx}^{(2)} = \chi_{s,xxz}^{(2)} = \chi_{s,xzx}^{(2)} &= N_S \langle \cos \theta \sin^2 \theta \rangle \langle \cos^2 \phi \rangle \alpha_{\zeta\zeta\zeta}^{(2)}, \\ \chi_{s,zyy}^{(2)} = \chi_{s,yyz}^{(2)} = \chi_{s,yzy}^{(2)} &= N_S \langle \cos \theta \sin^2 \theta \rangle \langle \sin^2 \phi \rangle \alpha_{\zeta\zeta\zeta}^{(2)}, \\ \chi_{s,zxz}^{(2)} = \chi_{s,zzx}^{(2)} = \chi_{s,xzz}^{(2)} &= -N_S \langle \cos^2 \theta \sin \theta \rangle \langle \cos \phi \rangle \alpha_{\zeta\zeta\zeta}^{(2)}, \\ \chi_{s,xyy}^{(2)} = \chi_{s,yxy}^{(2)} = \chi_{s,yyx}^{(2)} &= -N_S \langle \sin^3 \theta \rangle \langle \sin^2 \phi \cos \phi \rangle \alpha_{\zeta\zeta\zeta}^{(2)}, \end{aligned} \quad (6)$$

where the x is the symmetry axis. Experimentally, all these tensor elements can be determined by SHG with proper geometry and polarization combinations. Knowing these susceptibility elements, the molecular orientation distribution can be deduced.

Consider 8CB (Octa-cyanobiphenyl) monolayer on polyimide-coated substrate as an example. Figure 5 shows the result of SHG as a function of azimuthal rotation angle ϕ for p-in/p-out, s-in/p-out, s-in/s-out and p-in/s-out polarization combinations⁵. If the surface is unrubbed, the signal is azimuthal isotropic as expected. $\chi_{s,zzz}^{(2)}$, $\chi_{s,zxx}^{(2)}$ can be deduced from the data. Using Eq. (5) as well as the

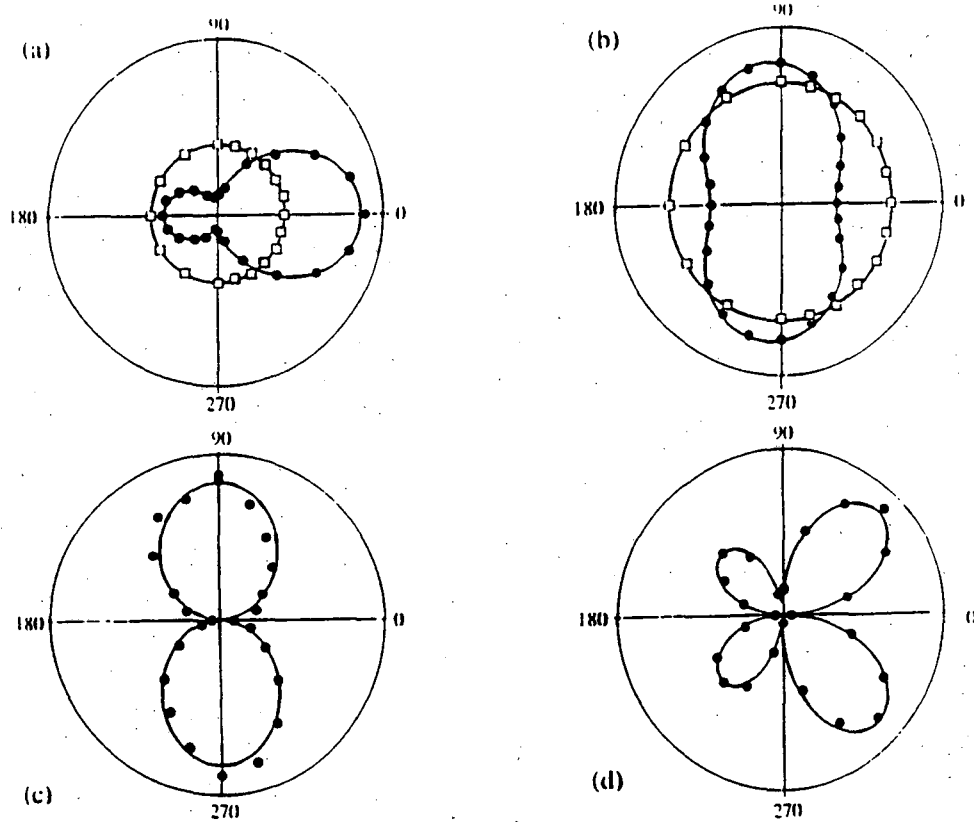


Fig. 5 Square root of second harmonic signal (arbitrary unit) vs sample rotation angle ϕ from an 8CB monolayer on rubbed and unrubbed polyimide-coated substrates. Open squares are data from unrubbed substrate, filled circles are data from substrate rubbed under a hard pressure, and solid lines are the theoretical fits. The input-output polarization combinations are (a) p-in/p-out; (b) s-in/p-out; (c) s-in/s-out; and (d) p-in/s-out. (After Ref. 5)

assumption of a δ -function orientation distribution in q , we obtain $q=72^\circ$. For the rubbed surface, the data clearly show the expected C_{1v} symmetry, from which the six independent $\chi_s^{(2)}$ elements can be deduced.

We can then assume a molecular orientation distribution with the functional form

$$f(\theta, \phi) \propto \exp\left(-\frac{(\theta - \theta_0)^2}{2\sigma^2}\right) \sum_{n=0}^3 d_n \cos(n\phi). \quad (7)$$

With $\chi_{s,ijk}^{(2)}$ known, Eq. (6) allows us to determine all the 6 coefficients in Eq. (7): $\theta_0=77^\circ$, $\sigma=5^\circ$, $d_1=0.167$, $d_2=0.762$, and $d_3=0.050$, the latter four yield the elongated azimuthal orientation distri-

bution shown as Fig. 6 (solid line).

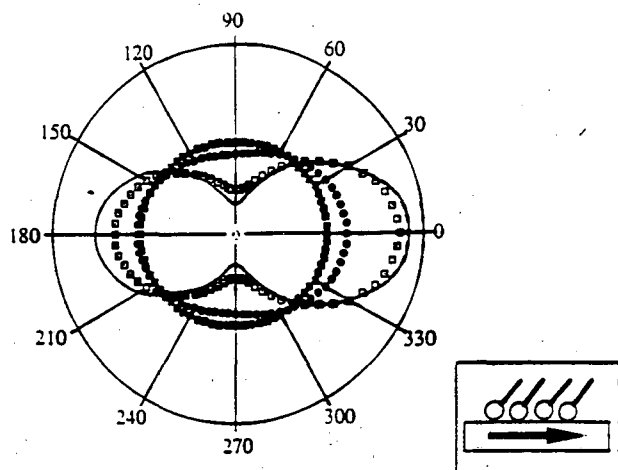
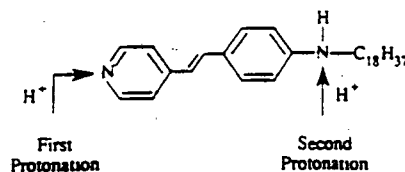


Fig. 6 Azimuthal orientational distribution functions of an 8CB monolayer on polyimide-coated substrates prepared with different rubbing strengths. The squares were for a sample prepared with a rubbing strength $R_s=1\gamma$, the circles were for $R_s=5\gamma$, the open squares were for $R_s=10\gamma$. The solid line corresponds to a sample rubbed with $R_s \gg 10\gamma$ (see Ref. 5 for definition of rubbing strength). Inset: Schematic of preferred orientation of molecular monolayer described by the orientational distribution function (After Ref. 5).

HEMICYANINE (HC):



NITROSTILBENE (NS):

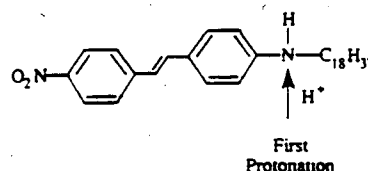


Fig. 7 Molecular structures of hemicyanine (HC) and nitrostilbene (NS) dyes. The arrows indicate the positions and the orders of protonation of the electron donor and acceptor groups (After Ref. 6).

Surface SHG can be sensitive to a surface chemical process if the change affects the surface nonlinearity. We consider here the case of protonation of molecular monolayer at the air/water interface. Protonation of the two molecules in Fig. 7 are expected to have substantial effect on their second order polarizabilities. In both molecules, nitrogen appears as the hetero atom in the substituent groups, i.e. the amino, pyridine, and nitro group. There are 5 valence electrons per nitrogen atom in the $3 sp^2$ orbitals parallel to the molecular plane and in the p_z orbital perpendicular to the plane. Electrons in the initial p_z orbital are delocalized as the orbital overlaps with the π -electron orbitals of the aromatic hydrocarbons. Depending on how the 5 electrons are distributed in these orbitals the nitrogen atom can play the role of either an electron donor or an electron acceptor. A detail analysis shows that the pyridine group is a strong electron acceptor and becomes even stronger upon protonation. The amino substituent, on the other hand, is an electron donor and loses its electron donating ability upon protonation. The nitro group appears as a significantly stronger electron acceptor than the pyridine nitrogen due to the stronger affinity of oxygen than both carbon and nitrogen.

For the hemicyanine (HC) molecule, protonation of the pyridine nitrogen enhance the electron delocalization and increases the second order polarizability. However, protonation of the amino nitrogen reduces the electron delocalization and decreases its second order polarizability. For nitrostilbene (NS) molecule, similar behavior upon protonation of the amino group is expected.

In the experiment, SHG from monolayers of HC and NS (diluted by steric acid) on water were measured⁶. Protonation of the molecules was varied by changing the bulk pH value of the water. The results are shown in Fig. 8. It is seen that the SH signal increases appreciably as the pyridine group of HC gets protonated with decreasing pH value. At very low pH values, the amino group also gets protonated and the SH signal decreases correspondingly. For NS, the amino group is first protonated, and therefore

the SH signal first decreases with decrease of bulk pH. From the measured surface nonlinearity $\chi_s^{(2)}$, it is possible to deduce the proton concentration at the air/water interface and hence the surface pH value.

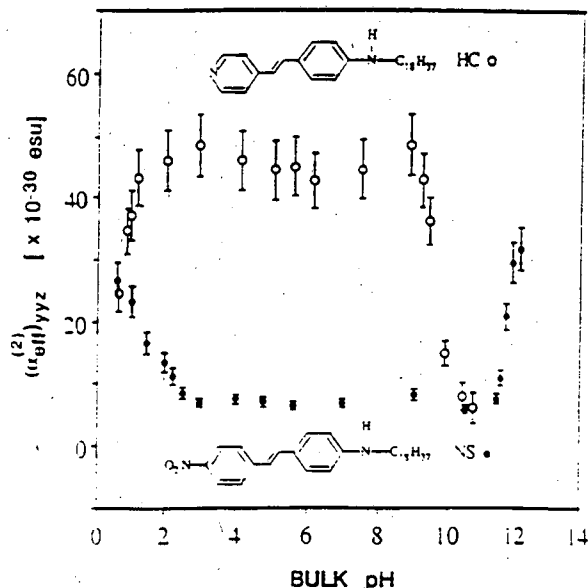


Fig. 8 Effective second-order polarizability $\alpha_{yyz}^{(2)}$ vs the bulk pH

for monolayers of hemicyanine (HC) and nitrostilbene (NS) embedded in a stearic acid matrix with a dye/stearic acid molar ratio of 1/15 and 1/6, respectively (After Ref. 6).

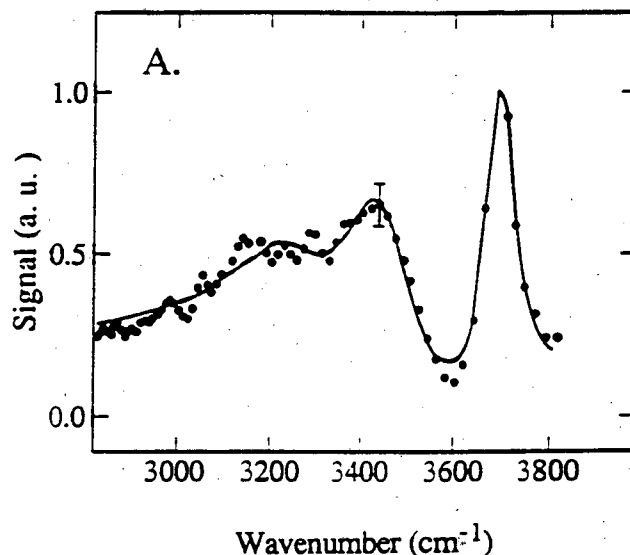


Fig. 9 SFG spectrum of pure water/vapor interface at 40°C

with polarization combination s, s, and p for the sum-frequency, visible, and infrared beams, respectively. Solid line is a theoretical fit (After Ref. 7).

IV. SPECTROSCOPY OF SURFACE STATES AND SURFACE ADSORBATES

Surface SHG can be a viable spectroscopy technique. In the visible-UV region, surface SHG has been used to study surface states. The advantage is that it can also probe buried interfaces on which photoemission spectroscopy is ineffective. The shortcoming is that it can only measure direct transitions.

Surface SFG is ideal for surface vibrational studies. Comparing to other spectroscopy techniques, it is also limited to measurements of direct transitions and is only sensitive to vibration modes that are both Raman and infrared active. Its advantage is the applicability to surfaces outside ultrahigh vacuum, its reasonable signal-to-noise ratio over infrared spectroscopy, and its enormous potential for transient spectroscopy and selective probing of ultrafast surface dynamics. An example of unique applications of SF surface vibrational spectroscopy is shown in Fig. 9, describing the OH stretch vibration of a pure water surface⁷. The existence of a free OH peak at $\sim 3700\text{cm}^{-1}$ indicates that the surface water molecules are polar orientated.

V. SUMMARY

In summary, we have briefly reviewed the possibility of using nonlinear optical techniques for surface studies. A number of examples have been given to illustrate the potential of the techniques. The field is still young. Improvement, extension, and many new applications of the techniques can be anticipated.

VI. ACKNOWLEDGEMENTS

The work presented in this paper were accomplished by a number of people who worked in Shen's group in Berkeley. The authors thank X. D. Zhu, Th. Raising, W. Daum for their contribution to CO/Ni adsorption and diffusion work; M. B. Feller, W. Chen for their contribution to the molecular orientation measurement; V. Vogel for her contribution on the protonation work, and Q. Du, R. Superfine, and E. Freysz for their contribution to SFG work. This work was supported by the Director, Office of Energy Research, Office of Basic Energy Sciences, Materials Sciences Division of the U.S. Department of Energy under Contract No. DE-ACO3-76SF00098.

VII. REFERENCES

1. Y. R. Shen, *Annu. Rev. Phys. Chem.* 40, 327(1989).
2. X. D. Zhu, Y. R. Shen and R. Carr, *Surf. Sci.* 163,114(1985).
3. X.-D. Xiao, X. D. Zhu, W. Daum, and Y. R. Shen, *Phys. Rev. B* 46, 9732(1992).
4. G. A. Reider, U. Höfer, and T. F. Heinz, *J. Chem. Phys.* 94, 4080(1991).
5. M. B. Feller, W. Chen, and Y. R. Shen, *Phys. Rev. a* 43, 6778(1991).
6. X.-D. Xiao, V. Vogel, and Y. R. Shen, *J. Chem Phys.* 94, 2315(1991).
7. Q. Du, R. Superfine, E. Freysz, and Y. R. Shen, preprints.

LAWRENCE BERKELEY LABORATORY
UNIVERSITY OF CALIFORNIA
TECHNICAL INFORMATION DEPARTMENT
BERKELEY, CALIFORNIA 94720